Available online at www.sciencedirect.com
SCIENCE DIRECT®
Journal of Solid State Chemistry 177 (2004) 1127–1136
JOURNAL OF SOLID STATE CHEMISTRY
http://elsevier.com/locate/jssc

The low-temperature structure of Tl_2SeO_4 at 30 K

K. Friese,[a,*] A.E. Goeta,[b] M.A. Leech,[b] J.A.K. Howard,[b] G. Madariaga,[c] J.M. Pérez-Mato,[c] and T. Breczewski[d]

[a] *Departamento de Física de la Materia Condensada, Universidad del País Vasco, Apdo. 644, Bilbao, Spain*
[b] *Chemistry Department, Science Site, Durham University, Durham DH1, 3LE, UK*
[c] *Departamento de Física de la Materia Condensada, Universidad del País Vasco, Apdo. 644, Bilbao, Spain*
[d] *Departamento de Física Aplicada II, Universidad del País Vasco, Apdo. 644, Bilbao, Spain*

Received 13 August 2003; received in revised form 7 October 2003; accepted 14 October 2003

Abstract

The structure of Tl_2SeO_4 at 293, 100 and 30 K has been determined. Space group at 293 and 100 K is *Pmcn*, $Z = 4$, lattice parameters at 293 K are $a = 6.0838(12)$(100 K: 6.0336(19)), $b = 10.965(3)$ (100 K: 10.903(5)) and $c = 7.9385(15)$ Å(100 K: 7.921(2)). At 30 K space group is $P2_12_12_1$, $Z = 4$, with lattice parameters $a = 6.2333(17)$, $b = 10.533(3)$ and $c = 7.828(2)$. Measurement was carried out with a Stoe IPDS (293 K) and a Nonius CCD using an Oxford He-cryostat for cooling (100 and 30 K). Final agreement factors at 293 K after refinement with the program SHELXL97 are $R(F) = 0.061$ (100 K: 0.097), $wR(F^{**}2) = 0.051$ (100 K: 0.156) for 566(100 K: 678) unique reflections and $R(F) = 0.039$, $wR(F^{**}2) = 0.097$ for 1162 unique reflections at 30 K. The high-temperature phase is isotypical to the β-K_2SO_4 structure, characterized by isolated selenate tetrahedra and two different cation sites with coordination number 9 and 11. In the low-temperature phase, the tetrahedra are rotated and the coordination numbers of the Tl^+ ions are reduced to 8 and 10, respectively. Structural changes are similar to the ones observed in high- and low-temperature phases of Tl_2MoO_4. A comparison to other Tl_2TX_4 compounds shows that the structural instabilities are closely connected to shortest Tl–O distances.

Keywords: Dithalliumselenate; Low-temperature phase; A_2BX_4 compounds; β-K_2SO_4; Glaserite; Phase transition

1. Introduction

A great number of compounds of general composition A_2TX_4 (with A, e.g., Na^+, K^+, Rb^+, Cs^+, Ca^{2+}, Sr^{2+}, Ba^{2+}, NH_4^+, Tl^+ crystallize in structures related to α-K_2SO_4 ([1]; space group $P6_3/mmc$)) which is characterized by isolated, orientationally disordered $[SO_4]^{2-}$-tetrahedra and two symmetrically independent A-cation sites. An illustration of the group–subgroup relationships between some relevant members of the family is given in Fig. 1.

The most prominent group of compounds which has been discussed in detail by Fábry and Pérez-Mato [2] crystallize in space group *Pmcn* with a pronounced hexagonal pseudosymmetry and a structure isotypical to β-K_2SO_4 [1,3]. Another important group are the structures which are isotypical to glaserite ($K_3Na(SO_4)_2$) and crystallize trigonal with space group $P\bar{3}m1$. The glaserite structure has three different A-cation sites which are normally occupied by two different A-cations depending on the size of the ions and the cavities formed within the structure respectively (the structure has been discussed in detail by Moore [4]).

In both structure types, phase transitions at high and low temperature do frequently occur. In the case of the compounds related to β-K_2SO_4, the most commonly observed mechanism for low-temperature phase transitions is characterized by the occurrence of an incommensurately modulated phase which locks-in to a phase with space group $P2_1cn$ and a tripled c lattice parameter (corresponding to the pseudohexagonal axis). In the case of the glaserite-related compounds, low-temperature phase transitions do normally lead to structures with symmetry $C2/c11$ or $C2/m11$.

*Corresponding author. Max-Planck Institut für Festkörperforschung, Heisenbergstr. 1, D-70569 Stuttgart, Germany. Fax: +49-711-689-1502.
E-mail address: k.friese@fkf.mpg.de (K. Friese).

0022-4596/$ - see front matter © 2003 Elsevier Inc. All rights reserved.
doi:10.1016/j.jssc.2003.10.020

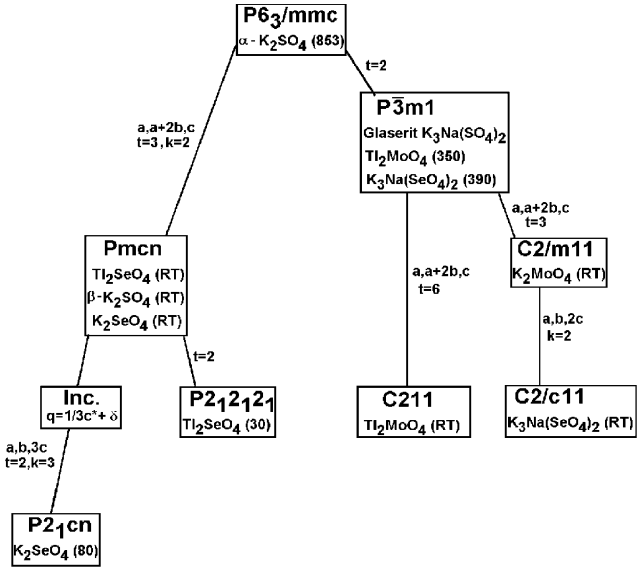

Fig. 1. Group–subgroup graph showing the relationship between some relevant A_2TX_4 compounds. Transformation for crystallographic axes and subgroup indexes (t = translationengleich, k = klassengleich; see [33]) are given; temperatures given in parenthesis, RT = room temperature; inc = incommensurate phase.

For the Tl_2TX_4 compounds the size of the tetrahedral T-cation is closely connected to the structure type formed. Thus, for the large cations W^{6+} and Mo^{6+} the glaserite structure is assumed while for the smaller cations the β-K_2SO_4 structure is preferred. The same is true for the K- and Rb-compounds as K_2MoO_4, K_2WO_4, Rb_2MoO_4 and Rb_2WO_4 assume also a glaserite-related structure (space group $C2/m11$) and the corresponding sulfates, selenates and chromates prefer the other branch of the group–subgroup tree and crystallize in structures related to β-K_2SO_4.

Yet, as far as structural phase transitions are concerned the Tl-bearing compounds of this family are rather exceptional and show a behavior which in many aspects is different from compounds of the family with other monovalent A-cations. This is probably an effect which is due to the lone-pair electron of Tl^+. A list of the Tl_2TX_4 compounds investigated so far, their space groups and lattice parameters are given in Table 1.

For Tl_2SO_4 and Tl_2CrO_4, the room-temperature phases have been refined [5,6] and it has been shown that they assume the β-K_2SO_4 structure which seems to be stable down to low temperatures. While Tl_2CrO_4 has one high-temperature phase transition at 782 K leading to a so far unknown structure, for Tl_2SO_4 no transition has been observed.

For the halogenide compounds Tl_2BeF_4 [7], Tl_2CoBr_4 [8], and Tl_2CoCl_4 [9–11], no detailed structural information is available. Anyhow, in the bromide one-phase transition at 451 K was found [9]. The authors assumed the space group $P2_1/m11$ for the room-temperature phase and space group $Pmcn$ for the high-temperature phase. In the fluoride and chloride, no phase transitions have been detected.

Tl_2MoO_4 is known to undergo three phase transitions at 311, 673 and 776 K [12] while for the Tl_2WO_4 no details are available. The room-temperature phase of Tl_2WO_4 [13] and the Tl_2MoO_4 phase in the temperature range between 311 and 673 K [14] are isotypical to the glaserite structure. The room-temperature phase of Tl_2MoO_4 crystallizes monoclinic, space group $C211$ [15].

According to literature, the title compound Tl_2SeO_4 possesses various phase transitions in the temperature range from 10 to 843 K where the crystals disintegrate. Contradictions exist as to the number of phase transitions and their corresponding temperatures. According to [12], three phase transitions above room temperature (at 428, 523 and 661 K, respectively) exist while later thermal and dielectric measurements indicate that there is only one anomaly close to a temperature of 661 K [16]. The low-temperature transition at approximately 70 K was first detected by Unruh [17]. In [18,19], this transition was further characterized by means of optical and X-ray powder measurements. The discontinuous change of the lattice parameters in the temperature range between 305 and 12.1 K indicates that the transition is of first order. Lattice parameters given by the authors at 25 K are $a = 6.2435(6)$ Å, $b = 10.5925(9)$ Å, $c = 7.8486(6)$ Å.

The room-temperature phase of Tl_2SeO_4 has been refined by Fábry [5] and the structure was shown to be isotypical to β-K_2SO_4. The space group is accordingly $Pmcn$ with lattice parameters $a = 6.086(2)$ Å, $b = 10.934(3)$ Å and $c = 7.927(2)$ Å.

The characterization of the low-temperature phase of Tl_2SeO_4 and its relationship to the high-temperature phase as well as to the other Tl-bearing compounds of the A_2TX_4 family was the aim of this work. Moreover, we were especially interested in a comparison with the low-temperature phase transition of K_2SeO_4 ($Pmcn \rightarrow$ incommensurate phase $\rightarrow P2_1cn$).

2. Experimental

The crystal used in this work was synthesized according to the method described in [5]. The diffraction intensities of Tl_2SeO_4 at room temperature were measured using a Stoe imaging plate (for details concerning the measurement see Table 2). At low temperatures (100 and 30 K), a Smart CCD in combination with an open He-cryostat from Oxford Cryosystem was used. The crystal was mounted on a glass pin and directly put into the He stream. Temperature was lowered to 100 K at a rate of 360 K/h. A first fast measurement was carried out at

Table 1
Space groups and lattice parameter of Tl_2TX_4 compounds

Compound	Space group	a (Å)	b (Å)	c (Å)	Refs.
Tl_2MoO_4, 350 K	$P\bar{3}m1$	6.266(1)		8.103(2)	[14]
Tl_2MoO_4	$C211$	6.4178(13)	10.565(3) $\alpha = 91.05(4)^\circ$	8.039(2)	[15]
Tl_2WO_4	$P\bar{3}m1$	6.278(1)		8.099(2)	[13]
Tl_2CrO_4	$Pmcn$	5.910(4)	10.727(6)	7.910(4)	[6]
Tl_2SO_4	$Pmcn$	5.934(7)	10.63(1)	7.821(5)	[29]
Tl_2SeO_4	$Pmcn$	6.086(2)	10.934(3)	7.927(2)	[5]
Tl_2SeO_4	$Pmcn$	6.0838(12)	10.965(3)	7.9385(15)	This work
Tl_2SeO_4, 100 K	$Pmcn$	6.0336(19)	10.903(5)	7.921(2)	This work
Tl_2SeO_4, 30 K	$P2_12_12_1$	6.2333(17)	10.533(3)	7.828(2)	This work
Tl_2BeF_4	?	5.87	10.43	7.68	[7]
Tl_2CoCl_4	?	7.182	12.635	9.131	[9]
Tl_2CoBr_4	?	7.520	13.145	9.424	[9]

Table 2
Experimental conditions and details concerning the structure refinement

Temperature	293 K	100 K	30 K
Space group	$Pmcn$	$Pmcn$	$P2_12_12_1$
a (Å)	6.0838(12)	6.0336(19)	6.2333(17)
b (Å)	10.965(3)	10.903(5)	10.533(3)
c (Å)	7.9385(15)	7.921(2)	7.828(2)
Reflections for lattice parameters	1649	1000	1000
V (Å^3)	529.6(2)	521.1(3)	513.9(2)
Formula weight		551.7	
$\rho_{calculated}$ (mg/m^3)	6.92	7.03	7.13
μ (mm^{-1})	67.56	68.65	69.61
Diffractometer	Stoe IPDS	SMART CCD	SMART CCD
Wavelength (Å)	0.71069	0.71069	0.71069
Number of frames	180	1800	1800
Increment (deg)	2 (ϕ)	0.3 (ω)	0.3(ω)
Exposure time (s)	60	20	45
θ range (deg)	3.2–26	3.2–28.6	3.2–28.5
hkl_{min}	$\bar{7}, \bar{13}, \bar{9}$	$\bar{8}, \bar{13}, \bar{10}$	$\bar{5}, \bar{13}, \bar{10}$
hkl_{max}	7, 13, 9	5, 12, 10	8, 7, 10
Absorption correction with program		Gaussian [30], X-RED [31]	
Crystal size (mm^3)		0.00296	
Crystal approximated by		21 faces	
T_{min}	0.0049	0.0047	0.0046
T_{max}	0.0317	0.031	0.031
Total number reflections	3544	2764	2460
Unique reflections	566	678	1162
Reflections $\geqslant 2\sigma$	369	491	1100
$R(F^2)_{int} = \sum \lvert F_o^2 - F_o^2(mean)\rvert / \sum [F_o^2]$	0.098	0.155	0.044
Structure refinement program		SHELXL97 [32]	
$R(F_{all}) = \sum \lvert F_o\rvert - \lvert F_c\rvert / \sum \lvert F_o\rvert$	0.061	0.097	0.039
$R(F_{observed})$	0.028	0.061	0.037
$wR(F^2_{all}) = \{\sum[w(F_o^2 - F_c^2)^2] / \sum[w(F_o^2)^2]\}^{1/2}$	0.051	0.156	0.097
$wR(F^2_{observed})$	0.047	0.139	0.096
Extinction correction		SHELXL97 [32]	
Extinction coefficient	0.00247(12)	0.0032(5)	0.0013(2)
Twinning matrix	—	—	$(-1, 0, 0/0, -1, 0/0, 0, -1)$
Volume fraction 2nd twin individual	—	—	0.40(5)
Diff. density maximum	1.757, 1.00 Å from O1	5.413, 0.80 Å from T12	3.008, 0.84 Å from T12
Diff. density minimum	−1.792	−3.050	−2.186
Weighting scheme with		$w = 1/[\sigma^2(F_{obs})^2 + (aP)^2 + bP]$, $P = (\mathrm{Max}(F^2_{obs}) + 2F^2_{calc})/3$	
a	0.0099	0.0611	0.0430
b	0.0	23.8676	26.3810

this temperature. Further lowering of temperature was slower with a rate of 30 K/h as preliminary experiments showed that the transition was rather violent and the crystals often broke down if the transition temperature was passed too fast. Measurement at 30 K was carried out with parameters given in Table 2. For the Gaussian absorption correction the crystal was approximated by 21 faces.

Structure refinement at all temperatures was carried out using the neutral atomic scattering factors, f' and f'' from [20] and the model coordinates from the work of [5]. At 293 and 100 K, the observed systematic extinctions led to the possible space groups *Pmcn* and $P2_1cn$. As refinement in the acentric space group did not lead to better agreement factors than the ones in *Pmcn*, it was discarded and space group *Pmcn* was assumed as the correct one for these temperatures.

At 30 K, an analysis of the extinction rules showed reflections violating the *c* and *n* glide plane of the high-temperature phase. The observed extinctions were in accordance with the three screw axis in the orthorhombic system indicating the space group $P2_12_12_1$. Anyhow, to be sure about the symmetry, refinement was also tried in space groups $P2_1/m11$, $P2_111$, $P12_11$, $P112_1$, $P\bar{1}$ and *P*1 symmetry. Refinement in $P2_1/m$ led to bad agreement factors, while for the other five space groups the agreement factors showed no significant improvement with respect to $P2_12_12_1$ and we therefore considered $P2_12_12_1$ to be the correct choice. During the refinement process, it became clear that the crystal was an inversion twin and consequently we introduced the corresponding twin law. The volume fraction of the second twin individual was refined to a value of 0.40(5). At this temperature, we were not able to refine the anisotropic displacement factors of the oxygen atoms which is due to the fact that the isotropic displacement factors are extremely small for these atoms and data do not reach up to sufficiently high θ angles to provide the necessary information.

Final agreement factors are given in Table 2, atomic coordinates and isotropic displacement parameters in Table 3. Important interatomic distances and angles are listed in Table 4.

Table 3
Positional and equivalent thermal displacement parameters (in Å^2) for Tl_2SeO_4 at 293, 100 and 30 K

Atom	*x*	*y*	*z*	U_{eq}
293 K				
Tl1	0.25	0.71619(8)	−0.00169(12)	0.0345(3)
Tl2	0.25	0.08357(9)	0.17172(12)	0.0349(3)
Se	0.25	0.4216(2)	0.2085(2)	0.0216(5)
O1	0.25	0.4232(18)	0.005(2)	0.066(5)
O2	0.25	0.5601(18)	0.282(2)	0.056(5)
O3	0.032(2)	0.3552(14)	0.2798(15)	0.055(4)
100 K				
Tl1	0.25	0.71500(13)	−0.0029(2)	0.0171(5)
Tl2	0.25	0.08242(14)	0.1694(2)	0.0166(5)
Se	0.25	0.4229(3)	0.2094(5)	0.0126(8)
O1	0.25	0.423(3)	0.000(3)	0.034(9)
O2	0.25	0.560(3)	0.285(5)	0.039(10)
O3	0.029(3)	0.357(2)	0.280(3)	0.027(5)
30 K				
Tl1	0.27661(12)	0.71633(6)	0.00655(9)	0.0065(2)
Tl2	0.27098(13)	0.08030(6)	0.17229(9)	0.0066(2)
Se	0.2412(3)	0.41672(16)	0.2067(2)	0.0058(4)
O1	0.173(2)	0.4449(15)	0.005(2)	0.013(3)
O2	0.297(2)	0.5537(13)	0.2989(18)	0.010(3)
O3a	0.033(3)	0.3494(16)	0.298(2)	0.012(3)
O3b	−0.047(3)	−0.3223(15)	−0.2220(19)	0.008(3)

3. Results and discussion

An examination of the *a*, *b* and *a*, *c* projection (Figs. 2 and 3) shows the drastic change in the structure of Tl_2SeO_4 which takes place when passing the transition temperature. While in the high-temperature phase the basal oxygen atoms of the tetrahedra are aligned in the (0 0 1) plane in the low-temperature phase the tetrahedra are rotated and three of the oxygen atoms are now nearly aligned in the (1 1 0) plane (see Fig. 2). Changes of similar importance have been observed in the phase transition at 311 K in Tl_2MoO_4 were the tetrahedra are rotated around the trigonal *a*-axis of the high-temperature phase (space group $P\bar{3}m1$) leading to a monoclinic phase with symmetry *C*211 [15].

Though the main structural change can be described via the rotation of the tetrahedra, it seems as if for the stability of the compounds the geometries of the tetrahedra are of minor importance. Thus, a close look at the $[TX_4]^{2-}$-tetrahedra in the selenate and the molybdate reveals that the average bond lengths in the low-temperature phases are increased (see Table 5). At the same time the shortest anion–anion contact in the selenate is lengthened (2.584(5) Å at 100 K compared to 2.652(5) Å at 30 K). Yet, the shortest O–O distance observed in the other Tl_2TX_4 compounds is 2.432 Å in Tl_2SO_4—a distance well below the sum of the ionic radii (2.80 Å)—and here no structural instability is observed. Also, there seems to be no correlation between the degree of distortion of the tetrahedra and the tendency to undergo phase transitions (see Table 6). The Tl_2SeO_4 has low BLDP and ELDP parameters (0.27% and 0.80%; for definition see [21]) and undergoes a phase transition, while the chromate and the sulfate have higher or comparable parameters and are stable. Furthermore, while the distortion of the tetrahedra in the Tl_2SeO_4 is relaxed after the phase transition, the opposite is true in Tl_2MoO_4 where the distortion is increased after the phase transition.

Table 4
Selected distances and angles for Tl_2SeO_4 at 293, 100 and 30 K

293 K			100 K			30 K		
Distance (Å)								
Tl1	O2	2.829(16)	Tl1	O2	2.84(3)	Tl1	O3b	2.727(16)
	O3	2.893(16)(2×)		O3	2.875(19)(2×)		O3a	2.834(17)
	O3	2.904(11)(2×)		O3	2.889(19)(2×)		O2	2.861(14)
	O2	2.994(16)		O2	2.97(3)		O1	2.931(17)
	O1	3.213(18)		O1	3.18(3)		O3b	2.933(16)
	O1	3.404(18)(2×)		O1	3.37(3)(2×)		O3a	2.952(17)
		3.049			3.030		O2	2.953(14)
							O1	3.000(17)
								2.899
Tl2	O1	2.647(18)	Tl2	O1	2.619( )	Tl2	O1	2.641(17)
	O3	3.060(12)(2×)		O3	3.006(19)(2×)		O2	2.717(14)
	O2	3.075(16)(2×)		O2	3.05(3)(2×)		O3b	2.817(16)
	O3	3.371(18)(2×)		O3	3.392(19)(2×)		O3a	3.092(17)
	O3	3.448(18)(2×)		O2	3.42(3)		O3a	3.260(17)
	O2	3.472(16)		O3	3.43(3)(2×)		O2	3.273(14)
	O1	3.952(18)		O1	3.95(3)		O3b	3.321(16)
		3.271			3.248		O3a	3.347(17)
							O2	3.559(17)
							O3a	3.928(17)
								3.200
Se	O3	1.613(12)(2×)	Se	O2	1.61(3)	Se	O3a	1.642(17)
	O1	1.618(19)		O3	1.615(19)(2×)		O2	1.650(14)
	O2	1.628(18)		O1	1.66(3)		O3b	1.657(16)
		1.618			1.625		O1	1.662(17)
								1.653
O1	O3	2.660(5)	O1	O3	2.686(5)	O1	O3a	2.652(5)
O1	O3	2.660(5)	O1	O3	2.686(5)	O1	O3b	2.757(5)
O1	O2	2.662(5)	O1	O2	2.707(5)	O1	O2	2.684(5)
O2	O3	2.609(5)	O2	O3	2.584(5)	O2	O3a	2.709(5)
O2	O3	2.609(5)	O2	O3	2.584(5)	O2	O3b	2.692(5)
O3	O3	2.653(5)	O3	O3	2.667(5)	O3a	O3b	2.700(5)
		2.642			2.652			2.699
Angle (*deg*)								
O3–Se–O3		110.3(10)	O3–Se–O3		111.1(15)	O3a–Se–O3b		109.8(8)
O3–Se–O1		110.8(5)(2×)	O3–Se–O1		110.3(10)(2×)	O3a–Se–O1		106.8(8)
						O3b–Se–O1		112.3(8)
O3–Se–O2		107.1(7)(2×)	O3–Se–O2		106.5(12)(2×)	O3a–Se–O2		110.8(8)
						O3b–Se–O2		108.9(8)
O1–Se–O2		110.5(9)	O1–Se–O2		112(2)	O1–Se–O2		108.3(7)
		109.4			109.5			109.5

But in both Tl_2SeO_4 and Tl_2MoO_4 the rotation of the tetrahedra is accompanied by an important change in the environment of the Tl^+ ions (see Fig. 4). Generally, the Tl-coordination number in the Tl_2TX_4 compounds is variable ranging from six to 12 and there is a linear relationship between coordination number and average Tl–O distance in the polyhedra. In both the selenate and the molybdate, the coordination number for the Tl^+ ions is reduced after the phase transition. To illustrate the changes in the Tl-coordination polyhedra of Tl_2SeO_4 they are drawn in detail in Fig. 4 (for a similar discussion of the molybdate see [15]). While in the high-temperature phase the coordination sphere of Tl1 is formed by nine oxygen atoms, in the low-temperature phase only eight oxygen atoms belong to the first coordination sphere and one of the O1 atoms is now at too long a distance. The coordination for Tl2 in the high-temperature phase can be described as 11. In the low-temperature phase, the most distant O1 atom is further away and the coordination number is decreased to 10. Unluckily, due to the rather complicated and irregular shape of the coordination polyhedra formed around the Tl^+- ions, it is difficult to figure out the location of the lone-pair electrons in the structures and practically impossible to describe the influence they have on the transition mechanisms.

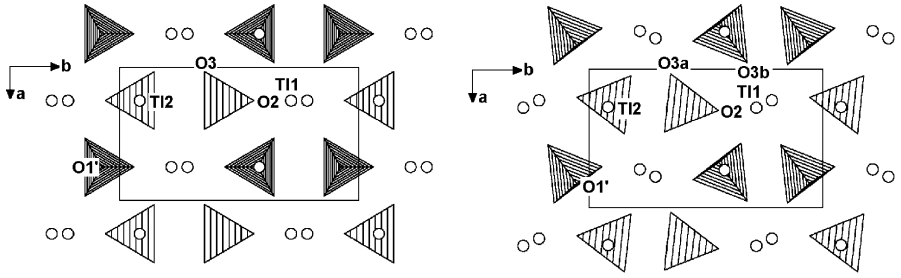

Fig. 2. a,b—projections of the structure of Tl_2SeO_4 at (left) 293 K and (right) 30 K. Selenate tetrahedra are shown; drawn with [34].

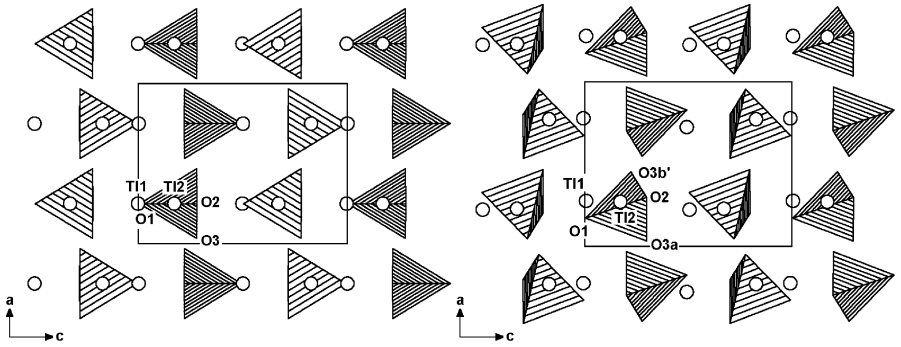

Fig. 3. a,c—projections of the structure of Tl_2SeO_4 at (left) 293 K and (right) 30 K. Selenate tetrahedra are shown; drawn with [34].

Table 5
Average bond distances in Å for the cation coordination polyhedra in Tl_2TX_4 compounds

Compound	T–X	Tl1–X	Tl2–X	Tl3–X	Refs.
Tl_2WO_4	1.775	2.699	3.292	3.242	[13]
Tl_2MoO_4, 350 K	1.719	2.769	3.282	3.258	[14]
Tl_2MoO_4	1.730	2.819	3.098	3.177	[15]
Tl_2CrO_4	1.682	2.926	3.207		[6]
Tl_2SO_4	1.501	3.012	3.157		[29]
Tl_2SeO_4	1.598	3.050	3.270		[5]
Tl_2SeO_4	1.618	3.049	3.271		This work
Tl_2SeO_4, 100 K	1.625	3.030	3.248		This work
Tl_2SeO_4, 30 K	1.653	2.899	3.200		This work

However, the stability of the compounds is clearly connected to the shortest Tl–O distances observed. In the molybdate this distance is 2.467(16) Å, in the selenate it is 2.619(19) Å at 100 K. In the other compounds (see Table 6)—with the exception of the tungstate—this distance is generally larger. Additionally, in both the selenate and the molybdate the transition leads to structural changes which lengthen this bond: for the molybdate it is 2.557(13) Å after the transition, for the selenate it is 2.641(17) Å. In the tungstate the shortest Tl–O distance observed is 2.456 Å and thus assumes a value even shorter than in the molybdate. If the length of this bond is really relevant for the structural stability this suggests that the tungstate should also undergo a low-temperature phase transition.

As was pointed out by Fábry and Pérez-Mato [2] in compounds isotypical to β-K_2SO_4 the A-cation in 11-fold coordination often shows "underbonding". This underbonding leads to structural instabilities and the subsequent occurrence of phase transitions. Looking at the Tl_2SeO_4 one sees that at room temperature the nine-fold coordinated Tl1 atom has a nearly ideal bond valence of 0.97 v.u., while the Tl2 with 11-fold coordination shows underbonding with a value of only 0.81 v.u. (see Table 6). The change of the coordination sphere for the Tl-atoms in Tl_2SeO_4 after the phase transition clearly improves the bond valence sums of especially the Tl2 ion (0.99 v.u.). The same is true for the molybdate where the phase transition also leads to an improve of the bond valence sums of the underbonded $Tl^{[12]}$ in the high-temperature phase (0.87 v.u.) to the more ideal value of 0.96 in the low-temperature phase. On the other hand, the stable sulphate shows a low value for $Tl^{[11]}$ (0.85 v.u.) also and makes clear that the underbonding does not necessarily lead to a structural instability.

To describe the structural distortion in Tl_2SeO_4 brought about by the phase transition in more detail we carried out a symmetry mode analysis (for details see [15,22–24]). The phase transition which is characterized by a symmetry change from $Pmcn$ to $P2_12_12_1$ involves nine different symmetry modes (see Table 7), four of which are primary (i.e., they have symmetry $P2_12_12_1$) while the remaining five modes are secondary (i.e., the symmetry is in accordance with $Pmcn$). The amplitudes

Table 6
Some crystal chemical data for Tl_2TX_4 compounds

Compound	Min (Tl–X)	Min (X–X)	$s(T)$	$s(A1)$	$s(A2)$	$s(A3)$	BLDP	ELDP	AD	Refs.
Tl_2WO_4	2.456	2.869	5.97	1.44 [6]	0.84 [12]	0.92 [10]	1.98	0.86	9.74	[13]
Tl_2MoO_4, 350 K	2.467	2.78	6.66	1.20 [6]	0.87 [12]	0.90 [10]	0.56	0.72	4.96	[14]
Tl_2MoO_4	2.557	2.780	6.49	1.08 [6]	0.96 [10]	0.96 [9]	1.97	1.36	5.61	[15]
Tl_2CrO_4	2.702	2.702	5.42	1.31 [9]	0.90 [11]		0.77	1.24	3.79	[6]
Tl_2SO_4	2.850	2.432	5.58	0.98 [9]	0.85 [11]		0.80	0.61	5.53	[29]
Tl_2SeO_4	2.66	2.575	6.66	0.96 [9]	0.80 [11]		0.89	0.97	3.08	[5]
Tl_2SeO_4	2.647	2.609	6.33	0.97 [9]	0.81 [11]		0.27	0.80	4.14	This work
Tl_2SeO_4, 100 K	2.619	2.584	6.23	1.01 [9]	0.87 [11]		1.05	1.65	5.32	This work
Tl_2SeO_4, 30 K	2.641	2.652	5.77	1.15 [8]	0.99 [10]		0.41	0.82	4.04	This work

Min$(Tl-X)$ = minimum Tl–anion bond distance; Min$(X-X)$ = minimum anion–anion distance; $s(T), s(A1), s(A2), s(A3)$ = bond valence sums for cations; coordination number for Tl atoms given in parenthesis; BLDP = bond length distortion parameter, ELDP = edge length distortion parameter for tetrahedra, AD = angular distortion [21]; BLDP $= \frac{100}{4}\sum_{i=1}^{4}(|(T-X)_i - \langle T-X\rangle_{\text{average}}|/\langle T-X\rangle_{\text{average}})\%$; ELDP $= \frac{100}{6}\sum_{i=1}^{6}(|(X-X)_i - \langle X-X\rangle_{\text{average}}|/\langle X-X\rangle_{\text{average}})\%$; AD $= 100\sum_{j=1}^{n}(|a_j|/4)\%$ with $a_j = 100\sum_{i=1}^{3}(|\alpha_i - \alpha_{\text{ideal}}|/\alpha_{\text{ideal}})\%$ where i runs over the three angles adjacent to each bond.

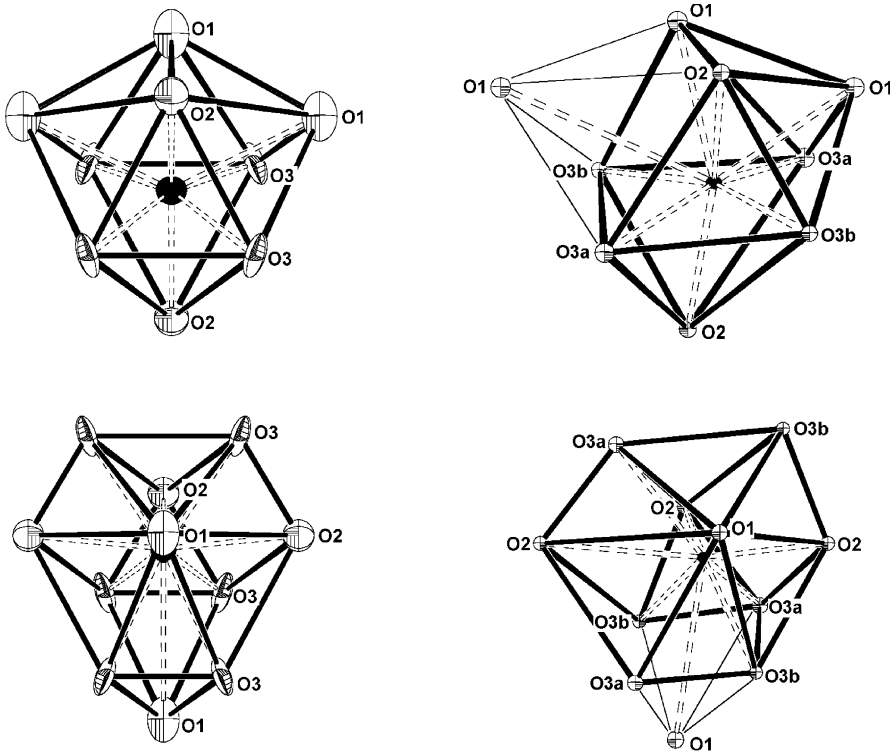

Fig. 4. The coordination polyhedra around the Tl atoms (left) in the high-temperature phase (293 K) and (right) in the low-temperature phase (30 K); view approximately along the pseudohexagonal axis [0$\bar{1}$0] (additional rotation of 6° around a-axis for reasons of clearness); the thermal ellipsoides are at 50% probability level; drawn with ORTEP-3 for Windows [35].

of the modes which have been calculated subtracting the coordinates of the low-temperature phase from the ones in the high-temperature phase are given in Table 8. As in the molybdate [15], the amplitudes are smallest for the tetrahedral cation and largest for the O-ions. One clearly sees the importance of the primary modes and the secondary modes are generally smaller. Yet, compared to the molybdate the secondary modes are far more important. Thus, in the selenate a refinement taking into account only the primary modes of the atoms results in an R-value of about 12% while the final refinement gives an R-value of 4%. In the molybdate, the R-value accounting for primary modes only is already 5% compared to 3% for the final result.

As Tl_2SeO_4 and K_2SeO_4 are isotypical at room temperature it is interesting to compare the corresponding low-temperature distortions in both compounds. The low-temperature $P2_1cn$ structure of K_2SeO_4 with a

Table 7
Chain adapted symmetry modes compatible with the symmetry $P2_12_12_1$ for atoms at Wyckoff positions 4c $(1/4, y, z)$ and 8d (x, y, z) of space group *Pmcn*

Atoms (4c)	*Pmcn*		$P2_12_12_1$			
	ϕ_1^y	ϕ_2^z	ϕ_3^x			
$1/4, y, z$	0 1 0	0 0 1	1 0 0			
$1/4, 1/2-y, 1/2+z$	0 $\bar{1}$ 0	0 0 1	$\bar{1}$ 0 0			
$3/4, 1/2+y, 1/2-z$	0 1 0	0 0 $\bar{1}$	$\bar{1}$ 0 0			
$3/4, -y, -z$	0 $\bar{1}$ 0	0 0 $\bar{1}$	1 0 0			
	1/2	1/2	1/2			
Atoms (8d)	*Pmcn*			$P2_12_12_1$		
	ϕ_4^x	ϕ_5^y	ϕ_6^z	ϕ_7^x	ϕ_8^y	ϕ_9^z
x, y, z	1 0 0	0 1 0	0 0 1	1 0 0	0 1 0	0 0 1
$1/2-x, 1/2-y, 1/2+z$	$\bar{1}$ 0 0	0 $\bar{1}$ 0	0 0 1	$\bar{1}$ 0 0	0 $\bar{1}$ 0	0 0 1
$-x, 1/2+y, 1/2-z$	$\bar{1}$ 0 0	0 1 0	0 0 $\bar{1}$	$\bar{1}$ 0 0	0 1 0	0 0 $\bar{1}$
$1/2+x, -y, -z$	1 0 0	0 $\bar{1}$ 0	0 0 $\bar{1}$	1 0 0	0 $\bar{1}$ 0	0 0 $\bar{1}$
$-x, -y, -z$	$\bar{1}$ 0 0	0 $\bar{1}$ 0	0 0 $\bar{1}$	1 0 0	0 1 0	0 0 1
$1/2+x, 1/2+y, 1/2-z$	1 0 0	0 1 0	0 0 $\bar{1}$	$\bar{1}$ 0 0	0 $\bar{1}$ 0	0 0 1
$x, 1/2-y, 1/2+z$	1 0 0	0 $\bar{1}$ 0	0 0 1	$\bar{1}$ 0 0	0 1 0	0 0 $\bar{1}$
$1/2-x, y, z$	$\bar{1}$ 0 0	0 1 0	0 0 1	1 0 0	0 $\bar{1}$ 0	0 0 $\bar{1}$
	1/4	1/4	1/4	1/4	1/4	1/4

Table 8
Amplitudes of the symmetry modes describing the $P2_12_12_1$ phase of Tl_2SeO_4 compared with the *Pmcn* room-temperature phase (amplitudes given in relative units)

Atom	*Pmcn*			$P2_12_12_1$		
	ϕ_1^y	ϕ_2^z		ϕ_3^x		
Tl1	−0.00014	−0.00824		−0.02661		
Tl2	0.00327	−0.00057		−0.02098		
Se	0.0048	0.0018		0.0088		
O1	−0.0217	0.0		0.077		
O2	0.0064	−0.0169		−0.047		
Atom	ϕ_4^x	ϕ_5^y	ϕ_6^z	ϕ_7^x	ϕ_8^y	ϕ_9^z
O3	−0.001	0.0058	−0.0182	0.015	−0.0329	−0.0578

tripled c lattice parameter with respect to its room-temperature phase results from the instability of an incommensurate displacive mode with wave vector $q = (\frac{1}{3}+\delta)c^*$ which locks-in to its commensurate value below 93 K [25]. This apparently different low-temperature configuration of potassium selenate which is representative for a large family of compounds may in fact be closely related to the situation observed in Tl_2SeO_4. It is remarkable that the unstable phonon branch in K_2SeO_4 has A_u symmetry at the Γ point of the Brillouin zone [26] and a frozen mode of this symmetry would indeed lead to a distorted structure with symmetry $P2_12_12_1$ as observed in Tl_2SeO_4. Moreover, at room temperature the soft phonon branch in K_2SeO_4 has its minimum at the Γ point and only at lower temperatures this minimum moves to a value of approximately $1/3c^*$ [26].

The question thus arises whether the primary structural distortion involved in the low-temperature phase transition of Tl_2SeO_4 (necessarily of symmetry A_u) can be related with the eigenvector of the soft mode in K_2SeO_4. This latter can be decomposed into two parts: the cosine part of symmetry B_{3g} (antisymmetric for the binary rotation around the x and y direction and their perpendicular mirror planes) and the sinus part of symmetry A_u (antisymmetric for the inversion and all mirror planes). This means that these cosine and sinus parts of the incommensurate modulation in K_2SeO_4 acquire B_{3g} and A_u symmetry, respectively, when their wave vector goes to zero. Hence, we can compare the amplitudes of the sinus component of the incommensurate modulation in potassium selenate with the primary distortion of Tl_2SeO_4 calculated above. As one should expect only a rough correlation of both systems, we can

neglect the small distortions of the $[SeO_4]^{2-}$ tetrahedra in both materials and compare only the "external" part of the modes. The displacements of the thallium and oxygen atoms in the primary mode given in Table 8 can indeed be fitted up to 7% to translations along x (Tx) and rotations around the y- and z-axis (Ry, Rz) of the $[SeO_4]^{2-}$ tetrahedra. The resulting A_u mode eigenvector is given by

$$\mathrm{Tl1}(x) = -0.02661,$$

$$\mathrm{Tl2}(x) = -0.02098,$$

$$\mathrm{SeO_4}\ (T\mathrm{x}) = 0.00682,$$

$$\mathrm{SeO_4}\ (R\mathrm{y}) = 19.98,$$

$$\mathrm{SeO_4}\ (R\mathrm{z}) = -7.29.$$

Here the rotations are given in degrees and the translation in relative units. The corresponding incommensurate mode in K_2SeO_4 at 113 K as given in Table 3 of [27] is (after transformation to the *Pmcn* setting and interchanging the cation labels):

$$\mathrm{K1}(x) = 0.0184/0.921,$$

$$\mathrm{K2}(x) = 0.0138/0.602,$$

$$\mathrm{SeO_4}\ (T\mathrm{x}) = 0.0116/0.325,$$

$$\mathrm{SeO_4}\ (R\mathrm{y}) = 7.36/0.143,$$

$$\mathrm{SeO_4}\ (R\mathrm{z}) = 4.54/0.536,$$

where the two values represent the modulus and the phase (in 2π units) of the corresponding complex amplitude. The sinus A_u component of the modulation is given by minus the imaginary part of these complex amplitudes:

$$\mathrm{K1}(x) = 0.01660,$$

$$\mathrm{K2}(x) = 0.00825,$$

$$\mathrm{SeO_4}\ (T\mathrm{x}) = -0.01034,$$

$$\mathrm{SeO_4}\ (R\mathrm{y}) = -5.76,$$

$$\mathrm{SeO_4}\ (R\mathrm{z}) = 1.02.$$

The global sign of the mode eigenvectors is arbitrary, hence a rough correlation of the mode A_u of Tl_2SeO_4 and the A_u part of the soft mode in K_2SeO_4 is observed. The relative signs of the amplitudes coincide and—in very broad terms—also the relative magnitudes. In the Tl compound, the translations of the monovalent cations with respect to the tetrahedra increase significantly and especially the amplitudes of the rotations of the $[SeO_4]^{2-}$ group are much larger, while the relative combination of y and z rotations of the same type is kept. This qualitative similarity between the modes in both compounds probably originates on pure general stereo hindrance for the atomic displacements associated with the common isotypic structure. Yet quantitatively the two modes differ much more than what has usually been detected in calculated or observed modes (with the same wave vector) for other A_2TX_4 compounds [27,28]. However, here we have compared the primary distortion of the Tl_2SeO_4 (for $q = 0$) with the K_2SeO_4 soft mode at $q = 1/3c^* + \delta$ (its part of A_u symmetry). But the A_u mode at $q = 0$ in K_2SeO_4 can in principle be quite different due to anti-crossings with other branches and will probably resemble more the frozen mode observed in the thallium compound.

Anyhow, it is reasonable to assume that the anisotropic interaction associated with the lone pair of the thallium cations—which is not present in the other A_2TX_4 compounds where the mode eigenvectors were investigated so far—can introduce a quite different dynamical scenario and may be the main factor for the observed discrepancies.

Acknowledgments

The authors gratefully acknowledge financial support by the Universidad del País Vasco (EB098/97), the Gobierno Vasco (PI97/71) and the Deutsche Forschungsgemeinschaft (Fr1332/2-1).

References

[1] H. Arnold, W. Kurtz, A. Richter-Zinnius, J. Bethke, G. Heger, Acta Crystallogr. B 37 (1981) 1643–1651.
[2] J. Fábry, J.M. Pérez-Mato, Phase Transitions 49 (1994) 193–229.
[3] K. Ojima, Y. Nishihata, A. Sawada, Acta Crystallogr. B 51 (1995) 287–293.
[4] P.B. Moore, Am. Min. 58 (1973) 32–42.
[5] J. Fábry, T. Breczewski, Acta Crystallogr. C 49 (1993) 1724–1727.
[6] R.L. Carter, T.N. Margulis, J. Solid State Chem. 5 (1972) 75–78.
[7] H. Arend, P. Muralt, S. Plesko, D. Altermatt, Ferroelectrics 24 (1980) 297–303.
[8] H. Kasano, S. Tsuchigama, H. Mashiyama, J. Korean Phys. Soc. 32 (1998) S53–S55.
[9] H.J. Seifert, L. Stäudel, Z. Anorg. Allg. Chem. 436 (1977) 105–107.
[10] F. Shimizu, M. Takashige, T. Yamaguchi, J. Korean Phys. Soc. 32 (1998) S21–S23.
[11] F. Shimizu, T. Kurihama, T. Yamaguchi, M. Takashige, Ferroelectrics 262 (2001) 1087–1092.
[12] M. Gaultier, G. Pannetier, Rev. Chim. Miner. 9 (1972) 271–289.
[13] K. Okada, J. Ossaka, Acta Crystallogr. B 35 (1979) 2189–2191.
[14] K. Friese, G. Madariaga, T. Breczewski, Acta Crystallogr. C 55 (1999) 1753–1755.
[15] K. Friese, M.I. Aroyo, C.L. Folcia, G. Madariaga, T. Breczewski, Acta Crystallogr. B 57 (2001) 142–150.
[16] Y. Matsuo, J. Hatori, K. Irokawa, M. Komukae, T. Osaka, Y. Makita, J. Phys. Soc. Jpn. 65 (1996) 3931–3934.
[17] H.G. Unruh, Ferroelectrics 25 (1980) 507–510.
[18] T. Grunwald, W. Hoffmann, P. Seidel, Ferroelectrics 55 (1984) 39–42.

[19] T. Grunwald, W. Hoffmann, P. Seidel, Ferroelectrics 56 (1984) 91–94.
[20] A.J.C. Wilson (Ed.), International Tables for Crystallography, Vol. C, Kluwer Academic Publishers, Dordrecht, 1992.
[21] B. Renner, G. Lehmann, Z. Kristallogr. 175 (1986) 43–59.
[22] J.M. Pérez-Mato, F. Gaztelua, G. Madariaga, M.J. Tello, J. Phys. C: Solid State Phys. 19 (1986) 1923–1935.
[23] A. Guleylah, M.I. Aroyo, J.M. Pérez-Mato, Phase Transitions 59 (1996) 155–179.
[24] J.M. Pérez-Mato, F.J. Zúñiga, G. Madariaga, Phase Transitions 16/17 (1989) 439–444.
[25] M. Izumi, J.D. Axe, G. Shirane, K. Shimaoka, Phys. Rev. B 15 (1977) 4392–4411.
[26] I. Etxebarria, M. Quilichini, J.M. Pérez-Mato, P. Boutrouillet, F.J. Zuñiga, T. Breczewski, Phys. Rev. 46 (1992) 2764–2774.
[27] I. Etxebarria, J.M. Pérez-Mato, G. Madariaga, Phys. Rev. 46 (1992) 2764–2774.
[28] J.M. Pérez-Mato, G. Madariaga, F.J. Zúñiga, Phase Transitions 16/17 (1989) 445–449.
[29] G. Pannetier, G. Gaultier, C. R. Hebd. Sean. Acad. Sci., Ser. C., Sci. Chim. 263 (1966) 132–134.
[30] P. Coppens, in: F.R. Ahmed, S. Hall, C.P. Huber (Eds.), Crystallographic Computing, Munksgaard, Copenhagen, 1970, pp. 255–270.
[31] STOE & CIE GmbH, X-RED: Data Reduction for STADI4 and IPDS, Computer Program, Darmstadt, Germany, 1998.
[32] G. Sheldrick, SHELXL97, a Program for Refining Crystal Structures, Computer Program, University of Göttingen, Germany, 1997.
[33] C. Hermann, Z. Kristallogr. 69 (1929) 533–555.
[34] R.X. Fischer, STRUPLO84, J. Appl. Crystallogr. 18 (1985) 258–262.
[35] L.J. Farrugia, ORTEP-3 for Windows, Computer Program, University of Glasgow, Scotland, UK, 1996.